Sensitivity Analysis of Thermodynamic Properties of Liquid Water: A General Approach to Improve Empirical Potentials†

Tzvetelin D. Iordanov, Gregory K. Schenter,* and Bruce C. Garrett*

Chemical Science Division, Pacific Northwest National Laboratory, P.O. Box 999, Mail Stop K1-83, Richland, Washington 99352

Received: July 14, 2005

A sensitivity analysis of bulk water thermodynamics is presented in an effort to understand the relation between qualitative features of molecular potentials and properties that they predict. The analysis is incorporated in molecular dynamics simulations and investigates the sensitivity of the Helmholtz free energy, internal energy, entropy, heat capacity, pressure, thermal pressure coefficient, and static dielectric constant to components of the potential rather than the parameters of a given functional form. The sensitivities of the properties are calculated with respect to the van der Waals repulsive and the attractive parts, plus short- and long-range Coulomb parts of three four site empirical water potentials: TIP4P, Dang−Chang and TTM2R. The polarization sensitivity is calculated for the polarizable Dang−Chang and TTM2R potentials. This new type of analysis allows direct comparisons of the sensitivities for different potentials that use different functional forms. The analysis indicates that all investigated properties are most sensitive to the van der Waals repulsive, the short-range Coulomb and the polarization components of the potentials. When polarization is included in the potentials, the magnitude of the sensitivity of the Helmholtz free energy, internal energy, and entropy with respect to this part of the potential is comparable in magnitude to the other electrostatic components. In addition similarities in trends of observed sensitivities for nonpolarizable and polarizable potentials lead to the conclusion that the complexity of the model is not of critical importance for the calculation of these thermodynamic properties for bulk water. The van der Waals attractive and the long-range Coulomb sensitivities are relatively small for the entropy, heat capacity, thermal pressure coefficient and the static dielectric constant, while small changes in any of the potential contributions will significantly affect the pressure. The analysis suggests a procedure for modification of the potentials to improve predictions of thermodynamic properties and we demonstrate this general approach for modifying potentials for one of the potentials.

1. Introduction

Water has been a subject of extensive experimental and theoretical studies. Many authors consider the original work of Bernal and Fowler[1] of the interpretation of X-ray data of liquid water structure as the beginning of modern theoretical studies of water. Over the years the research in this field has led to numerous fundamental discoveries.[2] Theoretical and computational studies have contributed significantly to our fundamental understanding of liquid water. A major limitation in the accuracy of results from simulations is the reliability of the underlying model of the interaction potential. Most potential models for water have been developed to reproduce experimentally measured properties of liquid water, although accurate theoretical results, particularly for cluster energetics, have played an increasing important role in the parametrization of potential models for water. Although many useful approaches have been suggested, the development of computationally efficient and accurate potential models that reproduce a wide variety of experimentally measured properties remains a challenging problem. The difficulty is associated not only with complexity and efficiency of the model but also with the availability of consistent as well as highly accurate experimental and theoretical data.

Many of the developed empirical models are based on simple analytical potentials parametrized to reproduce specific macroscopic properties. In each case there is significant computational effort used to fit the potential parameters. A model that is parametrized in such a way usually does not perform very well for some microscopic properties. For example the TIP5P[3] model gives excellent agreement with the experimental density, internal energy and OO radial distribution function at room temperature but overestimates the binding energy of the water dimer, although this property was included in the training set. Many water models fall into the family of nonpolarizable pairwise-additive models. These potentials are usually parametrized to reproduce the properties of liquid water and include the polarization response to the environment in a mean field sense. Often these models do not fully reproduce cluster properties[4−7] and provide a poor description of the liquid−vapor interface[8] as well as the interaction between nonpolar solutes and polar solvents.[9] The lack of mathematical complexity describing the proper physics and enough potential parameters allowing for more freedom in the fitting procedure makes the attempts to improve these models impractical.

Advanced models that include many-body polarization effects have a more complicated mathematical description and are capable of approximately modeling the physics of the polarization. Many recently developed polarizable models such as ASP−W2 and ASP−W4,[10] POL5/TZ and POL5/QZ,[11]

* To whom correspondence should be addressed. E-mail: (G.K.S.) greg.schenter@pnl.gov; (B.C.G.) bruce.garrett@pnl.gov.

† Part of the special issue "Donald G. Truhlar Festschrift".

10.1021/jp0538868 CCC: $33.50
Published on Web 10/18/2005

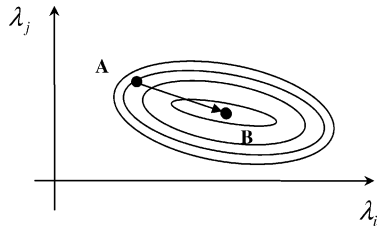

Figure 1. Contour of $|\mathscr{P}^{calc} - \mathscr{P}^{exp}|^2$. Illustration of parametrization differences. Point **A** corresponds to the original parametrization; point **B** corresponds to the new parametrization and λ_i, λ_j-are parameters of a model, $\mathscr{P}^{exp}$ and $\mathscr{P}^{calc}$ are the experimental and the calculated values for a given property, respectively.

AMOEBA,[12] TTM2R,[13] and TTM2F[14] use high level ab initio data as a basis to fit the potential parameters. High-level quantum mechanical data is currently available for clusters including up to 20 water molecules[15] and provides an important benchmark for ab initio based potentials. A complicating issue associated with these potentials is how quantum mechanical effects on nuclear motion are included. Empirical potentials that are fitted to experimental data are effective potentials that include quantum mechanical effects, such as zero-point energy constraints, in an implicit manner so that classical simulations reproduce experimental results. Potentials fitted to energetic data from ab initio calculations do not include these quantum mechanical effects and some properties, particularly ones associated with energies of the system, require quantum statistical mechanical simulations to ensure that calculate properties of water clusters and bulk water are accurate.

A common feature between all empirical potentials is the uncertainty in their parametrizations. To minimize the difference between calculated and experimentally measured properties (Figure 1) one could consider new parametrizations of existing potentials. This approach requires optimization searches in the multidimensional parameter space. The procedure is well-defined, but the execution can be complicated and inefficient due to existence of multiple sets of parameters that closely but incompletely satisfy the fitting requirements. Therefore, our goal is to search for a practical way to improve the theoretical results by developing a qualitative understanding of the relation between components of molecular potentials and the macroscopic properties that they predict. The sensitive part of a potential strongly influences the bulk properties and carries important physical information, which could suggest a practical way to improve the existing potential. The detailed characterization of a potential is provided by the sensitivity analysis.

Sensitivity analysis has been developed in the engineering field[16] to characterize uncertainties in input variables and model parameters. At present the methodology is also successfully used for a wide variety of complex physicochemical phenomena ranging from scattering problems[17] to protein folding.[18] Previously other groups have investigated the sensitivity analysis of liquid water. Zhu and Wong[19−21] have developed the combined sensitivity analysis/molecular dynamics method to study the sensitivity of structural and thermodynamic properties of bulk water. They have identified the most important parameters of the flexible SPC,[22] TIP3P,[23] and a newly developed polarizable water model based on parameters transferred from existing models. Antipova et al.[24] have explored the sensitivity of internal energy and structural properties of water as well. To our knowledge, these previous groups have not performed the sensitivity analysis with respect to parts of the empirical potential contributing to the specific type of interaction. A sensitivity analysis performed in such a manner allows for systematic examination and comparison of different empirical potentials in the effort to establish a practical way for improving parametrization procedures.

In this paper, we present a sensitivity analysis of the thermodynamic properties of liquid water and discuss a systematic parametrization method for empirical potentials. The analysis involves calculation of first-order sensitivity coefficients for a set of selected properties calculated using a sequence of water potentials ranging from a simple 4-point, nonpolarizable model (TIP4P), to a polarizable model (Dang−Chang) with a complexity similar to TIP4P, and finally to a polarizable model (TTM2R) with a more robust functional form. In addition, the TIP4P and Dang−Chang potentials were parametrized using experimental data, while the TTM2R potential is fitted to ab initio data for small water clusters. The water molecules are treated as rigid for all three potential models. The approach highlights the uncertainty in the parametrization of different parts of the potential instead of the specific potential parameters and enables direct comparison between potentials with different analytic forms. Furthermore, we use the information gained from the sensitivity analysis to demonstrate how a potential model based on ab initio data (e.g., TTM2R) can be modified in a straightforward way to be used in classical simulations of bulk water.

2. Theory

Sensitivity analysis measures the response of an observable to small perturbations of the potential parameters. The analytical forms of sensitivity coefficients are given by the partial derivatives in Taylor series expansion of an observable:

$$\mathscr{P} = \sum_i^N \frac{\partial \mathscr{P}}{\partial \lambda_i}\delta\lambda_i + \sum_i^N \sum_j^N \frac{\partial^2 \mathscr{P}}{\partial \lambda_i \partial \lambda_j}\delta\lambda_i\delta\lambda_j + ..., \qquad (1)$$

where N is the number of potential parameters λ_i. The first and second terms in the expansion correspond respectively to the first- and second-order sensitivity coefficients. In the current work, we decompose the potential energy based on the type of interactions and investigate the sensitivity of different thermodynamic properties with respect to different parts of the potentials. The potential is separated in the following way:

$$E_v = \lambda_{vdw,A}W_{vdw,A} + \lambda_{vdw,R}W_{vdw,R} + \lambda_{Coul,SR}W_{Coul,SR} + \lambda_{Coul,LR}W_{Coul,LR} + \lambda_P W_P \qquad (2)$$

Here E_v denotes the potential energy and W represents the different potential energy contributions. The notations vdw,A and vdw,R refer to van der Waals attractive and repulsive part of the potential, Coul,SR and Coul,LR refer to short- and long-range Coulomb interactions, and P refers to the polarization term. The λ_i parameters should not be confused with the actual potential parameters. All the λ_i's are constants equal to 1 and are used as a tool to separate different parts of the empirical potentials. The next section describes the manner of potential decomposition adopted in this work and summarizes the details of the sensitivity analysis of thermodynamic properties and the static dielectric constant.

2.1. Potential Decomposition. Weeks, Chandler, and Anderson[25] offered an elegant way to separate a van der Waals type of potential into repulsive and attractive contributions. According to the theory, the separation involves splitting of the potential at the minimum. Thus, for a Lennard-Jones potential:

$$W_{vdw}(r) = 4\epsilon\left(\left(\frac{\sigma}{r}\right)^{12} - \left(\frac{\sigma}{r}\right)^{6}\right) \qquad (3)$$

the corresponding parts are given by

$$W_{\mathrm{vdw,R}}(r) = \begin{cases} W_{\mathrm{vdw}}(r) + \epsilon & r < \sigma 2^{1/6} \\ 0 & r \geq \sigma 2^{1/6} \end{cases}$$
$$W_{\mathrm{vdw,A}}(r) = \begin{cases} -\epsilon & r < \sigma 2^{1/6} \\ W_{\mathrm{vdw}}(r) & r \geq \sigma 2^{1/6} \end{cases} \quad (4)$$

Here ϵ and σ are, respectively, the Lennard-Jones energy and radius. In this theory the molecules interact via a repulsive potential and represent the reference state and the attractive part is treated as a perturbation. The generality of the approach allows its application to different functional forms used to describe van der Waals interactions.

One of the most precise ways to treat long-range electrostatic terms in simulations of periodic systems is offered by the Ewald summation technique.[26] The approach describes the interaction of each particle with all periodic images of all particles, which effectively accounts for the electrostatic interaction in infinite systems. The technique is not limited to describing interactions between charges but can also be used for dipoles and higher order moments.[27] The generalization of the Ewald summation technique for potentials with atomic charges, dipoles and anisotropic polarizabilities has been presented as well.[28,29] Within the Ewald formalism the expression for the electrostatic potential energy is conveniently divided into a real term arising from the short-range interaction in real space, a reciprocal term arising from the long-range interaction in the reciprocal space, a self-term correction arising from over-counting in reciprocal space, a term representing the work of forming the induced dipoles, and a surface term, which appears only in systems with nonconducting boundary conditions. For the purposes of the sensitivity analysis, we define the Coulomb short-range contribution ($W_{\mathrm{Coul,SR}}$) from the charge−charge interaction in real space, and the long-range Coulomb contribution ($W_{\mathrm{Coul,LR}}$) that arises from the reciprocal space plus the contribution from the self-correction term by

$$W_{\mathrm{Coul,SR}} = \sum_{\mathbf{R}} \sum_{i<j} q_i q_j \frac{f(\kappa r_{ij})}{r_{ij}}$$
$$W_{\mathrm{Coul,LR}} = \sum_{\mathbf{R}} \sum_{i<j} q_i q_j \frac{1 - f(\kappa r_{ij})}{r_{ij}} \quad (5)$$

where q_i is the charge of atom i, $r_{ij} = |\mathbf{r}_i - \mathbf{r}_j - \mathbf{R}|$ is the distance between atoms i and j, $\mathbf{R}$ is the lattice parameter of periodically replicated systems, $f(\kappa r_{ij})$ is the complementary error function, and κ is the Ewald convergence parameter.

The polarization contribution (W_{P}) is defined as a sum between the work of forming the induced dipoles and the contributions arising from interactions such as charge−dipole and dipole−dipole in the periodic system

$$W_{\mathrm{P}} = \sum_i \frac{\mu_i^2}{2\alpha_i} + \sum_{\mathbf{R}} \sum_{i<j} (\mu_i \cdot \nabla_i q_j + q_i \mu_j \cdot \nabla_j + \mu_i \cdot \nabla_i \mu_j \cdot \nabla_j) \frac{1}{r_{ij}} \quad (6)$$

Here μ_i is the dipole moment of atom i and α_i is the polarizability of atom i. We separate the force and the virial coefficient in a similar manner.

2.2. Sensitivity Analysis. The conversion of the detailed microscopic information on a simulation into macroscopic terms can be done in any ensemble. Below we provide the equations necessary to perform the sensitivity analysis for a set of properties calculated in canonical ensemble. Different analytic expressions for the sensitivity coefficients are necessary in other ensembles. The properties of interest are the Helmholtz free energy, internal energy, entropy, heat capacity at constant volume, pressure, thermal pressure coefficient, and static dielectric constant. We define the Helmholtz free energy $A(N,V,T)$ in terms of the canonical ensemble partition function $Q(N,V,T)$:[30]

$$A(N,V,T) = -kT \ln Q = -\frac{1}{\beta} \ln \mathrm{Tr}[e^{-\beta \mathbf{H}}] \quad (7)$$

Here, $\mathbf{H}$ is the Hamiltonian of the system, $\beta = 1/k_{\mathrm{B}}T$, k_{B} denotes the Boltzmann constant, T is the temperature in kelvin, and Tr denotes a classical trace (integration in phase space). The first-order sensitivity coefficient is an ensemble average of the potential energy contribution corresponding to the given part of the potential:

$$\frac{\partial A}{\partial \lambda_i} = \langle W_i \rangle, \quad i = \{\mathrm{vdw,A;\ vdw,R;\ Coul,SR;\ Coul,LR;\ P}\} \quad (8)$$

Here the angular brackets refer to canonical ensemble average and the index refers to the corresponding potential contributions. The relation between the Helmholtz free energy and the partition function enables us to define many thermodynamic properties as first or higher order partial derivatives of the free energy with respect to the independent parameters of the canonical ensemble N, V or T. The entropy of a system is written as

$$S = -\left(\frac{\partial A}{\partial T}\right)_{N,V} \quad (9)$$

or defined from the following relation:[30]

$$A = U - TS \quad (10)$$

Here U is the internal energy of the system and is usually calculated as an ensemble average of the potential energy. The corresponding sensitivity coefficients for the internal energy and entropy are given by the following expressions:

$$\frac{\partial U}{\partial \lambda_i} = \langle W_i \rangle + \beta(\langle E_v \rangle \langle W_i \rangle - \langle E_v W_i \rangle) \quad (11)$$

$$T\frac{\partial S}{\partial \lambda_i} = \beta(\langle E_v \rangle \langle W_i \rangle - \langle E_v W_i \rangle) \quad (12)$$

where the ensemble average is defined by $\langle \cdots \rangle = \mathrm{Tr}[\cdots e^{-\beta \mathrm{H}}]/\mathrm{Tr}[e^{-\beta \mathrm{H}}]$, and E_v is the potential energy. The second partial derivative of the Helmholtz free energy with respect to the temperature provides the relation between the heat capacity and the free energy:

$$-\frac{1}{T}C_{\mathrm{v}} = \left(\frac{\partial^2 A}{\partial T^2}\right)_{N,V} \quad (13)$$

A convenient way to calculate the heat capacity is by using the fluctuations of the total energy.[31] For N rigid water molecules, the heat capacity at constant volume is given by the following expression:[32]

$$TC_{\mathrm{v}} = \beta(\langle E_v^2 \rangle - \langle E_v \rangle^2) + 3N\beta^{-1} \quad (14)$$

The kinetic contribution does not depend on λ_i and the corresponding sensitivity coefficient is defined as

$$T\frac{\partial C_v}{\partial \lambda_i} = \beta\langle(2E_v - \beta E_v^2)W_i\rangle + \beta^2\langle E_v^2\rangle\langle W_i\rangle - 2\beta\langle E_v\rangle\frac{\partial U}{\partial \lambda_i} \quad (15)$$

The thermodynamic definition of the pressure is based on the volume dependence of the Helmholtz free energy[30] $P = -(\partial A/\partial V)_{N,T}$ or it can be evaluated from the mechanistic prescription given by the virial theorem:

$$P = \langle P\rangle = \rho\beta^{-1} + \frac{1}{3V}\left\langle\sum_{i,j\neq i} r_{ij}\cdot f_{ij}\right\rangle \quad (16)$$

Here V is the volume of the simulation cell, ρ is the density, f_{ij} is the force on atom i due to atom j, and r_{ij} is the separation between these atoms. The thermodynamic pressure (P) can be defined as a parameter describing the ensemble, or an ensemble average of the instantaneous pressure (P), which is a mechanical property and should be distinguished from the thermodynamic concepts. Hummer et al. have shown that the virial pressure depends on system size, when less than 256 SPC/E[33] water molecules are used, while the thermodynamic pressure can be calculated accurately by using only 64 water molecules.[34] The kinetic part of the pressure in eq 16 is independent from the λ_i parameters, and therefore, the sensitivity coefficient is a derivative with respect to the part accounting for the intermolecular interactions

$$\frac{\partial P}{\partial \lambda_i} = \frac{1}{3V}\left\langle\sum_{i,j\neq i}^{N} r_{ij}\cdot\frac{\partial f_{ij}}{\partial \lambda_i}\right\rangle + \beta(P\langle W_i\rangle - \langle PW_i\rangle) \quad (17)$$

Analogously to the above properties, the thermal pressure coefficient is given as the mixed derivative of the Helmholtz free energy:

$$\gamma = \left(\frac{\partial^2 A}{\partial T\partial V}\right)_N \quad (18)$$

Combining the thermodynamic definition of pressure and eq 18, one sees that the thermal pressure coefficient measures the temperature dependence of the pressure. In *NVT* simulations the thermal pressure coefficient can be calculated from the following fluctuation formula:[31]

$$T\gamma = \beta\langle E_v P\rangle - \beta\langle E_v\rangle\langle P\rangle + \rho\beta^{-1} \quad (19)$$

The sensitivity coefficient is given by

$$T\frac{\partial \gamma}{\partial \lambda_i} = \beta\langle W_i P\rangle + \beta\left\langle\frac{1}{3V}\sum_{i<j} r_{ij}\frac{\partial f_{ij}}{\partial \lambda_i}E_v\right\rangle - \beta^2\langle E_v P W_i\rangle + \beta^2\langle E_v P\rangle\langle W_i\rangle - \beta\frac{\partial U}{\partial \lambda_i}P - \beta\frac{\partial P}{\partial \lambda_i}U \quad (20)$$

The static dielectric constant or permittivity ϵ_0 is calculated from fluctuations in the total dipole of the simulation cell. For a system with periodic boundaries and long-range electrostatic interactions treated by Ewald summation, ϵ_0 is given by[35]

$$\epsilon_0 = 1 + \frac{4\pi}{3k_B TV}(\langle M^2\rangle - \langle\mathbf{M}\rangle\cdot\langle\mathbf{M}\rangle) \quad (21)$$

For long simulation time the ensemble average of the total cell dipole for disordered liquids approaches zero and the term $\langle\mathbf{M}\rangle\cdot\langle\mathbf{M}\rangle$ can be neglected. Then the expression for the sensitivity coefficient is reduced to

$$\frac{\partial \epsilon_0}{\partial \lambda_i} = \frac{4\pi\beta^2}{3V}(\langle M^2\rangle\langle W_i\rangle - \langle M^2 W_i\rangle) \quad (22)$$

3. Potential Models and Simulation Details

In this work we use the following rigid four site empirical water potentials: TIP4P,[23] Dang−Chang,[36] and TTM2R.[13] The monomer geometry is the same for these models but the analytical forms of the potentials differ significantly (Table 1.). Both TIP4P and Dang−Chang models use the Lennard-Jones potential to model the van der Waals interactions as well as point charges for the hydrogen atoms and the M site. The main difference between these two potentials is the isotropic polarizability that the Dang−Chang potential carries on the M site to describe nonadditive polarization effects. The Thole-type model, TTM2R, significantly differs from the previous two potentials. The TTM2R uses a 12−10−6 polynomial to model the van der Waals interactions. The model uses smeared charges instead of point charges and isotropic atomic polarizabilities are assigned to the oxygen and hydrogen atoms.

Molecular dynamics simulations of a cubic box with side length L, containing 256 water molecules with periodic boundary conditions was employed to mimic the bulk water behavior. The Nose−Hoover thermostat[37,38] was used in the constant volume simulations at 298 K with a density of 0.997 g/cm^3. The cutoff distance for the van der Waals interactions was set to 50 Å. The electrostatic interactions were treated using the Ewald summation, with real space sum truncated at $L/2$, and 2221 **k**-vectors were considered in the reciprocal space. The "tin-foil boundary conditions" were assumed for the surrounding media and the value of the Ewald coefficient controlling the width of the Gaussian screening charges was 0.42 Å^{-1}. The convergence tolerance for the induced dipoles was 10^{-6} D and the integration of the rigid body equations of motion was done with velocity Verlet[39] algorithm and RATTLE[40] procedure with a 2.0 fs time step. After 200 ps of equilibration, all the runs were continued for an additional 10^6 time steps. We have used the variance of the mean to estimate the statistical error. For this purpose the entire trajectory was separated into 10 equal segments each corresponding to 200 ps of real time.

4. Results and Discussion

This section presents a sensitivity analysis of the thermodynamic properties of liquid water for three empirical water potentials and discusses the relation between the different components of these potentials and the calculated properties. The sensitivity analysis of phase equilibrium properties as well as time dependent properties such as diffusion coefficient is the goal of future work.

4.1. Sensitivity Analysis. Table 2 summarizes the sensitivity coefficients of the Helmholtz free energy with respect to different parts of the potentials. The coefficients are an ensemble average of the potential energy contributions resulting from the related part of the molecular potential (eq 8). Therefore, we expect similarities in the trends of free energy sensitivities with the trends in the internal energy sensitivities. The repulsive part of the van der Waals (VdW) and short-range Coulomb sensitivities show more noticeable differences among different potentials. The repulsive wall of the VdW potential has similar sensitivity for Dang−Chang and TTM2R models but they are slightly higher in comparison to the sensitivities of TIP4P potential. In this way the parametrization procedure has accounted for the higher net electrostatic contribution in the polarizable models compared to the nonpolarizable mode. The sensitivities with

TABLE 1: Monomer Geometries and Parameters for Potential Functions

	TIP4P	Dang−Chang	TTM2R
r(OH),Å	0.9572	0.9572	0.9572
∠HOH, deg	104.52	104.52	104.52
q(O), e	0.0	0.0	0.0
q(H), e	0.52	0.519	0.574
q(M), e	−1.04	−1.038	−1.148
r(OM), Å	0.15	0.215	0.25
A, Å^{12} kcal/mol	600.0×10^3	9.55439×10^5	-1.1954×10^6
C, Å^6 kcal/mol	610.0	8.35147×10^2	-2.0418×10^3
B, Å^{10} kcal/mol			3.3642×10^5
α(O), Å^3			0.837
α(H), Å^3			0.496
α(M), Å^3		1.444	

respect to the attractive VdW part also show noticeable differences, where the sensitivity for TTM2R is higher probably due to the different functional form used to describe the VdW in TTM2R. Overall the van der Waals sensitivities are similar and this suggests a consistency in the parametrizations of the selected potentials. The lower sensitivities for the attractive VdW suggest that this contribution is less significant. The differences between the short-range Coulomb sensitivity coefficients are more pronounced. The values for polarizable models appear to be smaller but if we add the sensitivities for the polarization piece to the short-range ones, the net sensitivity for the short-range electrostatics has a magnitude comparable to the TIP4P short-range sensitivity. Although Dang−Chang and TTM2R potentials use different analytical forms, the similarities in the sensitivity coefficients show a consistency in the parametrization of the potentials and suggest that the complexity of the model is not of critical importance for the calculation of the Helmholtz free energy of bulk water. Nevertheless, the polarization contribution appears to be very important and containing roughly 30% of the total electrostatic contribution to the potential energy and thus must be considered in situations when the model needs to respond adequately to the environment. The long-range Coulomb interaction appears to be less important. The sensitivities are several times smaller than the corresponding sensitivities for the short-range Coulomb interactions and their magnitude is within close range.

The sensitivities of the internal energy are reported in Table 3. The trends are like those reported for the Helmholtz free energy, and it should be noted that the magnitudes of the corresponding Helmholtz and the internal energy sensitivity coefficients are comparable. This suggests that it is reasonable to parametrize an empirical potential only with respect to one of these properties. The calculation of the Helmholtz free energy requires additional computational effort, which would increase the computational effort if it were used in the parametrization. It is reasonable that most models are parametrized to reproduce the internal energy instead of the free energy. Increasing the contribution of the VdW attraction and the electrostatic interactions will result in a lower internal energy while increasing the VdW repulsion will raise the corresponding value. Higher repulsive interactions will lead to a higher energy, and higher attractive interactions will lower the energy. This finding is in agreement with physical intuition and supports the validity of the analysis.

The sensitivity of the entropy to the potential contributions is reported in Table 4. Because of the relationship of the entropy to the free energy and enthalpy (eq 10), the sensitivity of the entropy should follow the trends observed for the previous two properties and they provide more of a consistency check. In agreement with the trend observed for the previous two properties, the attractive VdW, and the long-range Coulomb interactions are of minor importance. The sensitivity of the entropy to changes in these interactions is very low. In contrast, the sensitivity with respect to the repulsive VdW and the short-range electrostatic interactions are significantly larger. The entropy exhibits particularly high sensitivity to the short-range Coulomb term. The analysis suggests that increasing the short-range electrostatic contribution will lower the entropy. This behavior is consistent with the observed lowering of the internal energy. A similar effect could be achieved by decreasing the repulsive VdW contribution. It is interesting to note that for the Dang−Chang and TTM2R potentials the sensitivity of the entropy to changes in the polarization is again almost 30% of the total electrostatic sensitivity. The sensitivities for the TTM2R models are consistently lower for all the contributions compared to the corresponding values for TIP4P and Dang−Chang potentials, yet the coefficients are of comparable magnitude. We can conclude that the complexity of the functional form of the model is not crucial for the estimation of this property as well.

The heat capacity is a property often related to hydrophobic effects.[41,42] Some authors have also associated this property to the process of changing the structure of water and have used this property to classify solutes into structure making and structure breaking categories.[43] The correlation between the amount of disorder and heat capacity at constant volume is clearly demonstrated in the results in Table 5. In comparison with the sensitivity analysis of the entropy, the heat capacity exhibits stronger sensitivity with respect to changes in the repulsive VdW, short-range Coulomb and polarization interactions. The attractive part of the VdW and the long-range Coulomb sensitivities are, yet again, negligible for all models and the polarization contribution is again nearly one-third of the total electrostatic sensitivity. The similarities in the trends of the sensitivity analysis for both entropy and heat capacity at constant volume suggest that a potential parametrized to reproduce the experimental values for one of the properties is likely to improve the second one as well. In fitting a potential to the heat capacity, one should keep in mind that its value depends on the different boundary conditions and simulation protocols. Nevertheless, calculation of the heat capacity is free of the difficulties associated with the calculation of the free energy and entropy.

The pressure sensitivity coefficients reported in Table 6 are considerably larger than the other coefficients up to this point. This finding is consistent with large uncertainties in computed pressures because of the small sample sizes used in simulations. Small variations in any of the λ_i parameters will drastically change the pressure. Consistent with the findings from previously reported sensitivity analysis[20] of bulk water as well as the studies of Clementi[44] and co-workers, the intermolecular repulsion plays a key role in determining the pressure. Increasing the repulsive VdW contribution will amplify the pressure, while the increase in the attractive VdW and the electrostatic contributions will result in a pressure decrease. Similar to the internal energy, a fine balance between all the potential contributions is necessary to achieve adequate results for the liquid pressure. The similarity could be due to energetic effects related to the strength of the hydrogen bonds. This is in agreement with the smaller sensitivity of the pressure with respect to the long-range Coulomb and the high, roughly 50% of the net electrostatic interaction, sensitivity to changes in the polarization contribution.

From Table 7, it is evident that the repulsive VdW and the short-range electrostatic contributions affect the temperature dependence of the pressure the most. These interactions are

TABLE 2: Helmoltz Free Energy Sensitivity Coefficients in kcal mol^{-1}

	$(1/N)(\partial A/\partial\lambda_i)$				
	vdw,R	vdw,A	Coul,SR	Coul,LR	polarization
TIP4P	2.97 ± 0.00	−1.21 ± 0.00	−9.62 ± 0.01	−2.03 ± 0.00	0.00
Dang−Chang	4.12 ± 0.00	−1.55 ± 0.00	−7.34 ± 0.00	−1.56 ± 0.00	−3.19 ± 0.00
TTM2R	4.00 ± 0.00	−2.84 ± 0.00	−7.44 ± 0.00	−1.67 ± 0.00	−3.36 ± 0.00

TABLE 3: Sensitivity Coefficients of the Internal Energy in kcal mol^{-1}

	$(1/N)(\partial U/\partial\lambda_i)$				
	vdw,R	vdw,A	Coul,SR	Coul,LR	polarization
TIP4P	4.47 ± 0.04	−1.17 ± 0.00	−15.13 ± 0.11	−2.23 ± 0.00	0.00
Dang−Chang	7.06 ± 0.06	−1.51 ± 0.00	−12.24 ± 0.08	−1.73 ± 0.00	−5.93 ± 0.04
TTM2R	5.59 ± 0.05	−2.83 ± 0.00	−11.30 ± 0.05	−1.84 ± 0.00	−5.35 ± 0.03

TABLE 4: Sensitivity Coefficients of the Entropy in cal mol^{-1} K^{-1}

	$(1/N)(\partial S/\partial\lambda_i)$				
	vdw,R	vdw,A	Coul,SR	Coul,LR	polarization
TIP4P	5.05 ± 0.15	0.15 ± 0.01	−18.49 ± 0.36	−0.67 ± 0.01	0.00
Dang−Chang	9.88 ± 0.19	0.15 ± 0.01	−16.47 ± 0.25	−0.57 ± 0.01	−9.19 ± 0.12
TTM2R	5.32 ± 0.18	0.04 ± 0.01	−12.96 ± 0.16	−0.58 ± 0.01	−6.69 ± 0.11

TABLE 5: Sensitivity Coefficients of the Heat Capacity at Constant Volume in cal mol^{-1} K^{-1}

	$(1/N)(\partial c_v/\partial\lambda_i)$				
	vdw,R	vdw,A	Coul,SR	Coul,LR	polarization
TIP4P	−25.81 ± 7.23	−0.88 ± 0.23	71.04 ± 15.18	0.90 ± 0.63	0.00
Dang−Chang	−25.97 ± 9.68	−0.05 ± 0.30	23.79 ± 9.80	−0.44 ± 0.43	16.37 ± 8.19
TTM2R	−7.33 ± 4.48	−0.76 ± 0.41	4.39 ± 7.89	0.00 ± 0.91	5.04 ± 4.90

TABLE 6: Sensitivity Coefficients of the Pressure in atm

	$\partial P/\partial\lambda_i$				
	vdw,R	vdw,A	Coul,SR	Coul,LR	polarization
TIP4P	6017.7 ±184.8	−3122.1 ± 7.4	−5669.2 ± 332.1	−618.8 ± 13.0	0.00
Dang−Chang	9370.8 ± 356.2	−3991.7 ± 8.6	−4350.2 ± 242.5	−438.8 ± 8.9	−4348.6 ± 188.8
TTM2R	8730.0 ± 407.8	−7070.6 ± 10.1	−2951.3 ± 404.8	−506.8 ± 10.7	−2607.4 ± 279.2

TABLE 7: Sensitivity Coefficients of the Thermal Pressure Coefficient in atm K^{-1}

	$\partial\gamma/\partial\lambda_i$				
	vdw,R	vdw,A	Coul,SR	Coul,LR	polarization
TIP4P	17.79 ± 34.24	2.69 ± 0.66	−63.13 ± 38.96	−2.39 ± 3.77	0.00
Dang−Chang	−2.71 ± 41.19	2.87 ± 1.03	−63.69 ± 45.41	−4.86 ± 2.84	1.6 ± 27.09
TTM2R	78.64 ± 50.10	3.39 ± 1.02	−78.76 ± 38.39	−1.61 ± 1.71	−50.42 ± 26.33

TABLE 8: Sensitivity Coefficients of the Static Dielectric Constant

	$\partial\epsilon_0/\partial\lambda_i$				
	vdw,R	vdw,A	Coul,SR	Coul,LR	polarization
TIP4P	13.75 ± 34.25	0.12 ± 1.15	4.80 ± 67.14	2.00 ± 1.80	0.00
Dang−Chang	156.61 ± 114.24	1.55 ± 4.01	−224.19 ± 137.89	−1.26 ± 2.65	95.32 ± 104.83
TTM2R	26.08 ± 55.26	−0.68 ± 1.16	−38.24 ± 66.37	1.59 ± 1.76	3.66 ± 36.70

strongly correlated with the strength of the hydrogen bonds. Therefore, in calculations of the thermal pressure coefficient with flexible water models the role of molecular flexibility is accentuated.[20] The sensitivities for the thermal pressure coefficient reveal that the attractive VdW and the long-range Coulomb parts of the rigid potentials are less important. The high error bars indicate that the data is correlated and thus it is uncertain how significant polarization is compared to the short-range Coulomb contribution. The sensitivities of the thermal pressure coefficient show similar trend to the entropy and heat capacity. Nevertheless, the pressure and the thermal pressure coefficient show that stronger repulsion results in a higher and stronger response of the pressure to changes in the temperature.

Sensitivities of the static dielectric constants are shown in Table 8. The calculation of the static dielectric constant requires long simulations and proper treatment of the electrostatic interactions and the uncertainties in the computed values are relatively high (see Table 9). Table 8 shows that the uncertainties in the sensitivity coefficients often exceed the value of the sensitivity coefficient. Similar to the entropy, heat capacity, and thermal pressure coefficient, the static dielectric constant is highly sensitive to changes in the repulsive VdW, short-range Coulomb, and polarization interactions. These nearest-neighbor interactions account for reorientation of water molecules, affecting the level of molecular alignment and therefore system dipole fluctuation. The attractive VdW and long-range Coulomb sensitivities of the dielectric constant are relatively small.

4.2. Refining Model Potentials. The sensitivity results discussed above provide information that can aid in the refinement of potentials to provide closer agreement between

TABLE 9: Experimental and Calculated Values for the Internal Energy, Heat Capacity at Constant Volume, Pressure, Thermal Pressure Coefficient, and Static Dielectric Constant

model	U (kcal/mol)	C_v (cal/mol K)	P (atm)	γ (atm/K)	ϵ_0
experiment	-9.92[a]	17.9[a]	1.0	4.4[b]	78.36[c]
TIP4P	-9.89 ± 0.00	19.93 ± 1.95	72.9 ($\pm$ 6.7	11.63 ± 0.69	54.42 ± 3.03
Dang−Chang	-9.52 ± 0.00	22.17 ± 1.94	726.2 ± 9.1	15.07 ± 0.53	127.60 ± 10.13
TTM2R	-11.29 ± 0.00	20.83 ± 1.94	-1752.3 ± 10.4	8.90 ± 1.03	80.89 ± 4.13
adjusted model	-9.89 ± 0.00	19.29 ± 2.15	-231.2 ± 9.1	16.74 ± 0.81	81.52 ± 2.63

[a] Reference 2. [b] The value for the thermal pressure coefficient is estimated using the relation $\gamma = \alpha/\kappa_T$, where the thermal expansion coefficient α is 2.0×10^{-4} K^{-1} [47] and the isothermal compressibility κ_T is 45.8×10^{-6} atm^{-1} (ref 47). [c] Reference 48.

experimental values and those obtained from classical simulations. For this purpose we choose a set of observables to test our ability to parametrize potentials. In our training set we include internal energy (U), heat capacity at constant volume (C_v), pressure (P), thermal pressure coefficient (γ), and static dielectric constant (ϵ_0). Comparisons of the computed and experimental values for these properties are shown in Table 9 for the three potentials (TIP4P, Dang−Chang, and TTM2R) and a modification of one of the potentials (labeled adjusted model), which is discussed below. Most of the calculated results are in good agreement with the corresponding experimental values. The internal energy calculated with TTM2R potential is lower than experiment[2] but as discussed above, this difference is to be expected since the potential is parametrized to reproduce the ab initio data (D_e) and thus the internal energy computed from the current classical simulation does not take into account zero-point energy corrections. The polarizable potentials slightly overestimate the heat capacity at constant volume. More accurate calculations of the heat capacity require quantum simulation[45] or a quantum correction of the heat capacity, which can be derived from the classical counterpart of the quantum correlation function through velocity correlation functions.[46] The thermal pressure coefficient is consistently overestimated by all potentials compared to experiment.[47] The experimental static dielectric constant[48] is underestimated by TIP4P and overestimated by Dang−Chang, but the TTM2R agrees quite well.

In the sensitivity analysis we assume that all the λ_i coefficients are equal to one. To improve the prediction of a certain property we can change the value of λ_i to obtain better estimates of the experimental properties. An adjusted model potential is obtained from eq 2 with values of $\lambda \neq 1$. The procedure of just adjusting the values of λ_i is not recommended for generating new potential but for use in simulations to test how variations in the different components of the potential affect the computed properties and to identify which parts of the potential could benefit from reparametrization or from new functional forms. In addition, the adjusted potential can have discontinuous derivatives. The van der Waals potential as defined in eq 4 is continuous as a function of r for any values of $\lambda_{vdw,R}$ and $\lambda_{vdw,A}$, but its derivatives are only continuous when $\lambda_{vdw,R} = \lambda_{vdw,A}$. We performed a limited number of simulations for $\lambda \neq 1$ (discussed below) and found that the discontinuity in the derivatives did not cause any numerical problems in practice.

Optimum values of λ_i can be obtained according to the following set of linear equations:

$$\mathscr{P}_k^{exp} = \mathscr{P}_k^{calc} + \sum_i \frac{\partial \mathscr{P}_k}{\partial \lambda_i} \delta\lambda_i \tag{23}$$

Here denotes the corresponding observable in the training set $k = \{U, C_v, P, \gamma, \epsilon_0\}$. A qualitative analysis based on this expression reveals correlation between the properties. For example, increasing the VdW repulsive component of the potential will increase the computed dielectric constant for the TIP4P potential bringing it into better agreement with experiment, but it will increase the computed internal energy (make it less negative) degrading the agreement with experiment. Similar examples can be found for the rest of the properties in the training set. The property correlation makes the multidimensional search for potential parameters a demanding task requiring a robust fitting procedure to find the optimal values of λ_i. Using the least-squares method we define the following fitting function:

$$\chi^2 = \sum_k \left(\mathscr{P}_k^{exp} - \mathscr{P}_k^{calc}(\lambda) - \sum_i \delta\lambda_i \frac{\partial \mathscr{P}_k^{calc}(\lambda)}{\partial \lambda_i} \right)^2 w_k \tag{24}$$

where the weighting factor w_k can be defined as the inverse sum of the statistical error of the corresponding sensitivity coefficient:

$$w_k = \frac{1}{\sum_{j'} \sigma_{kj'}^2} \tag{25}$$

The derivative of the calculated observable with respect to the λ_i parameters represents the sensitivity coefficients defined in eq 1 and the values for $\delta\lambda_i$ can be found from the set of equations:

$$\frac{\partial \chi^2}{\partial \lambda_j} = -2 \sum_k \left(\mathscr{P}_k^{exp} - \mathscr{P}_k^{calc}(\lambda) - \sum_i \delta\lambda_i \frac{\partial \mathscr{P}_k^{calc}(\lambda)}{\partial \lambda_i} \right) \frac{\partial \mathscr{P}_k^{calc}(\lambda)}{\partial \lambda_j} w_k = 0 \tag{26}$$

For the two polarizable potentials the number of properties and unknowns is equal (five) and the solution to eq 26 is equivalent to that for eq 23. We solved eq 26 for the two polarizable potentials to give the following predicted values for the scaling of the different components that is needed to reproduce the experimental results:

Dang−Chang: $\lambda_{vdw,R} = 1.132$, $\lambda_{vdw,A} = 1.635$, $\lambda_{Coul,SR} = 1.182$, $\lambda_{Coul,LR} = 1.003$, $\lambda_p = 0.686$

TTM2R: $\lambda_{vdw,R} = 4.102$, $\lambda_{vdw,A} = 3.864$, $\lambda_{Coul,SR} = 2.783$, $\lambda_{Coul,LR} = -13.84$, $\lambda_p = 3.809$

It is not surprising that the Dang−Chang potential yields values of λ_i with smaller deviations from unity than TTM2R, because Dang−Chang was fitted so that classical simulations reproduced some of these properties whereas TTM2R is fitted to ab initio data to be consistent with quantum statistical mechanical simulations. The analysis does indicate that reducing the polarization

component, while increasing the short-range repulsive and coulomb components, of the Dang−Chang potential could improve the agreement with small number of properties studied here. The changes in the λ_i values for the TTM2R potential are so large that they are well outside the region where the linear approximation inherent in eq 23 is valid. Therefore, we can draw no conclusions from this analysis for the TTM2R potential. To obtain a better fit with the least-squares procedure, one should solve eq 26 with more properties than unknowns (λ's). Inclusion of other properties such as distribution functions or time dependent properties is the goal of future research.

As a further demonstration of how the sensitivities can be used to explore the effects of variations in potential components on computed properties, we examined the TTM2R potential in more detail. This potential was chosen because, as discussed above, it was fitted to ab initio electronic structure information, and properties such as the internal energy require quantum mechanical simulations to reproduce experimental values. We examined whether adjustments of the λ_i values to give an adjusted model, which reproduces the experimental internal energy in classical simulations, would yield a model potential that when used in classical simulations would reproduce other properties.

We used eq 23 to evaluate the corresponding variations of the λ_i values to give a computed internal energy that is in agreement with the experimental value. An infinite number of solutions to eq 23 exist for a single property. For this demonstration, we limited the search to the solution for which each term in the sum of eq 23 contributes equally to correcting the computed internal energy, which is equivalent to searching along the vector with components. Two simulations were performed for different values of λ_i to arrive at a reasonably good estimate for the internal energy. The adjusted model potential differs from the original potential by the following scaling parameters: $\lambda_{\mathrm{vdw,R}} = 1.057$, $\lambda_{\mathrm{vdw,A}} = 0.888$, $\lambda_{\mathrm{Coul,SR}} = 0.972$, $\lambda_{\mathrm{Coul,LR}} = 0.826$, and $\lambda_{\mathrm{P}} = 0.941$, and the values of U, C_{v}, P, γ, and ϵ_0 computed for this adjusted potential are shown in Table 9. Note that the linear relationship in eq 23 predicts the following values for U, C_{v}, P, γ, and ϵ_0 for these values of λ: −9.67 kcal mol^{-1}, 20.0 cal mol^{-1} K^{-1}, −119 atm, 18.9 atm K^{-1}, and 83.2, respectively. The good agreement between these linearly extrapolated values and those computed for the adjusted potential shows the validity of the linear approximation in eq 23 for the relatively small changes in λ_i values in this adjustment.

Table 9 shows that the adjusted model significantly improves the theoretical results for the internal energy (by construction) and the pressure, while the results for the heat capacity and the dielectric constant are within the error bars of the original potential. The agreement for the thermal pressure coefficient is much worse, but comparable to the value obtained using the Dang−Chang potential. We also calculated the radial distribution function (RDF) for the OO separation with the adjusted model and compare the OO RDF with those for the TTM2R potential, which agrees well with experiment, in Figure 2. The adjustment of the λ_i values also results in some deterioration of the OO radial distribution function (Figure 2). The structure is not lost but modified. The potential as a function of OO separation for the water dimer is shown in Figure 3. For each OO distance the geometry of the dimer was optimized without constraining the symmetry. The adjusted model exhibits the same behavior as the TTM2R potential, which is known to accurately reproduce high-level ab initio results. The kink on both curves is a result of changing the symmetry of the dimer from C_i to C_s and is in good agreement with previously reported

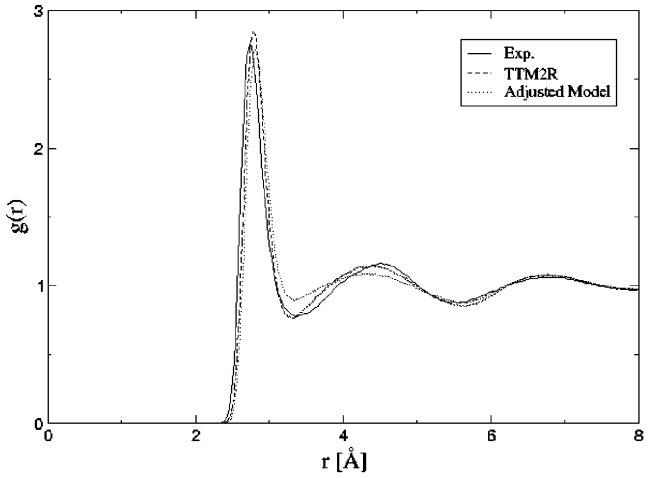

Figure 2. OO radial distribution function for the adjusted model, compared with results from the TTM2R potential and experiment.

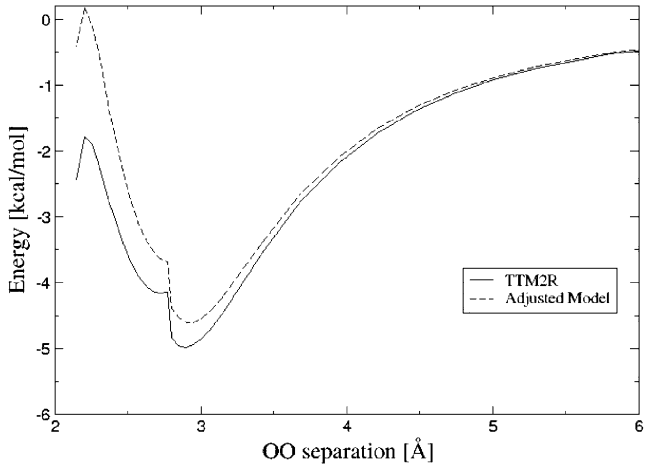

Figure 3. Potential energy for the water dimer interaction as a function of intermolecular O−O separation for TTM2R potential and the adjusted model. The geometry is optimized for each O−O distance with no constraint on symmetry.

results.[13] The adjusted model has its minimum at the same OO separation as the TTM2R potential and an energy that is shifted up by about 0.4 kcal/mol, which is in the correct direction toward the zero-point corrected value of the dimer energy (∼2.9 kcal/mol).[49,50] We emphasize that the adjusted model is not a complete potential and that our goal was not to generate a new potential but instead to search for a general approach that can serve as a tool to guide refinements to potentials. In future applications of this approach it will be useful to include more properties, such as the radial distribution function and time-dependent quantities, in the training set.

5. Conclusions

This paper presents a sensitivity analysis of bulk water properties, in an effort to understand the relation between components of molecular potentials and the properties that they predict. The pairwise additive TIP4P and polarizable Dang−Chang and TTM2R potentials were used in this analysis to find a systematic way to guide adjustments to existing potentials to improve their properties. All three potentials treat water as rigid with similar molecular geometries, but use different analytic forms for the water−water interaction. The decomposition of the potentials into van der Waals repulsive and attractive, Coulomb short- and long-range, and polarization terms enables

the comparison of potentials with different analytical forms and emphasizes the analysis of property sensitivity with respect to different parts of the potentials instead of the specific potential parameters. This approach reduces the dimensionality of the problem and can be used to guide adjustments to existing potentials (either by reparametrization or using new functional forms) to improve the agreement between computed properties and experimental results.

The sensitivity analysis suggests that all the investigated properties are more sensitive to changes in the short-range (VdW repulsive and short-range Coulomb) components for all three potentials to changes in the polarization component for the Dang−Chang and TTM2R potentials. The sensitivities for the Helmholtz free energy and the internal energy show similarities and the complexity of the model is not of critical importance for the calculation of these properties for bulk water. Consequently, only one of these properties could be used in the training set required in fitting procedures.

The sensitivities of the entropy and the heat capacity at constant volume reveal similarities as well. The VdW attractive and long-range Coulomb sensitivities are negligible for both the entropy and heat capacity. Therefore, only the entropy or only the heat capacity is sufficient to be included in the training set. The sensitivities of the Helmholtz free energy, internal energy, entropy, and heat capacity at constant volume to changes in the polarization component are nearly 30% of the total electrostatic sensitivity when the polarizable potentials are used.

The relation between short-range nearest-neighbor interactions and structure is strongly pronounced in the sensitivity of the pressure and thermal pressure coefficients. The repulsive VdW, short-range Coulomb, and polarizability contributions dominate the sensitivities of pressure and the thermal pressure coefficient. The polarization sensitivity to the pressure is approximately 50% of the total electrostatic contribution. A high sensitivity to polarizability is also demonstrated in the sensitivity of the static dielectric constant. This results from the strong influence of polarization interactions on the level of molecular alignment and therefore the fluctuation of the system dipole.

Adjustment the values of λ_i (from their value of 1) can we used to modify the magnitude of the contributions from the different components and yield an adjusted model potential. The model potential can be used to test how variations in the different components of the potential affect the computed properties and to identify which parts of the potential could benefit from reparametrization or from new functional forms. We used this adjustment procedure to examine whether the TTM2R potential, which was fitted to ab initio data for small water clusters and is most appropriate for quantum statistical mechanical simulations, could be modified to reproduce experimental bulk properties using classical simulations. The hope is that extensions of this potential fitted to a more complete set of experimental measurements will be able to reproduce structural and energetic properties of water clusters as well. Although the functional complexity of the model may not be important for simulation of some bulk water properties,[51] polarizability effects are important for the description of the liquid−vapor interface as well as the interaction between nonpolar solutes and polar solvents. Therefore, an adapted model based on the TTM2R potential could be a reasonable compromise between water models appropriate mostly for quantum simulations and simple nonpolarizable models appropriate for classical simulations of bulk properties.

Acknowledgment. This work was supported by the Division of Chemical Sciences, Office of Basic Energy Sciences, of the U.S. Department of Energy (DOE). This research was performed in part using the Molecular Science Computing Facility (MSCF) in the William R. Wiley Environmental Molecular Sciences Laboratory at the Pacific Northwest National Laboratory. The MSCF is funded by the Office of Biological and Environmental Research in the U.S. Department of Energy. Battelle operates Pacific Northwest National Laboratory for the DOE. The authors thank Dr. Shawn Kathmann and Dr. Liem Dang for many helpful discussions and Dr. George S. Fanourgakis and Dr. Sotiris S. Xantheas for generously providing software and useful discussions.

References and Notes

(1) Bernal, J. D.; Fowler, R. H. *J. Chem. Phys.* **1933**, *1*, 515.
(2) Eisenberg, D.; Kauzmann, W. In *The Structure and Properties of Water*; Oxford University Press: New York and Oxford, U.K., 1969.
(3) Mahoney, M. W.; Jorgensen, W. L. *J. Chem. Phys.* **2000**, *112*, 8910.
(4) Xantheas, S. S.; Burnham, C. J.; Harrison, R. J. *J. Chem. Phys.* **2002**, *116*, 1493.
(5) Perera, L.; Berkowitz, M. L. *J. Chem. Phys.* **1991**, *95*, 1954.
(6) Jorgensen, W. L.; Severance, D. L. *J. Chem. Phys.* **1993**, *99*, 4233.
(7) Perera, L.; Berkowitz, M. L. *J. Chem. Phys.* **1991**, *99*, 4236.
(8) Wilson, Michael A.; Pohorille, A.; Pratt, L. R. *J. Chem. Phys.* **1987**, *91*, 4873.
(9) van Belle, D.; Wodak, S. J. *J. Am. Chem. Soc.* **1993**, *115*, 647.
(10) Millot, C.; Soetens, J. C.; Costa, M. T. C. M.; Hodges, M. P.; Stone, A. J. *J. Phys. Chem. A* **1998**, *102*, 754.
(11) Stern, H. A.; Rittner, F.; Berne, B. J.; Friesner, R. A. *J. Chem. Phys.* **2001**, *115*, 2237.
(12) Ren, P.; Ponder, J. W. *J. Phys. Chem. B* **2003**, *107*, 5933.
(13) Burnham, C. J.; Xantheas, S. S. *J. Chem. Phys.* **2002**, *116*, 1500.
(14) Burnham, C. J.; Xantheas, S. S. *J. Chem. Phys.* **2002**, *116*, 5115.
(15) Fanourgakis, G. S.; Apra, E.; Xantheas, S. S. *J. Chem. Phys.* **2004**, *121*, 2655.
(16) Tomovick, R.; Vukobratovic, M. *General Sensitivity Theory*; American Elsevier: New York, 1972.
(17) Padmavathi, D. A.; Mishra, M. K.; Rabitz, H. *Phys. Rev. A* **1993**, *48*, 286.
(18) Bleil, R. E.; Wong, C. F.; Rabitz, H. *J. Phys. Chem.* **1995**, *99*, 3379.
(19) Zhu, S. B.; Wong, C. F. *J. Phys. Chem.* **1994**, *98*, 4695.
(20) Zhu, S. B.; Wong, C. F. *J. Chem. Phys.* **1993**, *98*, 8892.
(21) Zhu, S. B.; Wong, C. F. *J. Chem. Phys.* **1993**, *99*, 9047.
(22) Berendsen, H. J. C.; Postma, J. P. M.; vanGunsteren, W. F.; Hermans, J. *Intermolecular Forces*; Reidel: Dordrecht, The Netherlands, 1981.
(23) Jorgensen, W. L.; Chandrasekhar, J.; Madura, J. D.; Impey, R. W.; Klein, M. L. *J. Chem. Phys.* **1983**, *79*, 926.
(24) Antipova, M. L.; Petrenko, V. E.; Kessler, Y. M. *Russ. Chem. Bull.* **2003**, *52*, 330.
(25) Weeks, J. D.; Chandler, D.; Andersen, H. C. *J. Chem. Phys.* **1971**, *54*, 5237.
(26) Ewald, P. P. *Ann. Phys. (Leipzig)* **1921**, *64*, 253.
(27) Smith, W. *CCP5 Newslett.* **1998**, *46*.
(28) Toukmaji, A.; Sagui, C.; Board, J.; Darden, T. *J. Chem. Phys.* **2000**, *113*, 10913.
(29) Nymand, T. M.; Linse, P. *J. Chem. Phys.* **2000**, *112*, 6152.
(30) McQuarrie, D. A. *Statistical Mechanics*; University Science Books: Sausalito, CA, 2000.
(31) Allen, M. P.; Tildesley, D. J. *Computer Simulations of Liquids*; Clarendon Press: Oxford, U.K., 2002.
(32) Han, K.; Hale, B. N. *Phys. Rev. B* **1992**, *45*, 29.
(33) Berendsen, H. J. C.; Grigera, J. R.; Straatsma, T. P. *J. Phys. Chem.* **1987**, *91*, 6269.
(34) Hummer, G.; Gronbech-Jensen, N.; Neumann, M. *J. Chem. Phys.* **1998**, *109*, 2791.
(35) Neumann, M.; Steinhauser, O.; Pawley, G. S. *Mol. Phys.* **1984**, *52*, 97.
(36) Dang, L. X.; Chang, T. M. *J. Chem. Phys.* **1997**, *106*, 8149.
(37) Nose, S. *J. Chem. Phys.* **1984**, *81*, 511.
(38) Hoover, W. G. *Phys. Rev. A* **1985**, *31*, 1695.
(39) Swope, W. C.; Andersen, H. C.; Berens, P. H.; Wilson, K. R. *J. Chem. Phys.* **1982**, *76*, 637.
(40) Andersen, H. C. *J. Comput. Phys.* **1983**, *52*, 24.
(41) Gill, S. J.; Dec, S. F.; Olofsson, G.; Wados, I. *J. Phys. Chem.* **1985**, *89*, 3758.

(42) Arthur, J. W.; Haymet, A. D. J. *J. Chem. Phys.* **1999**, *110*, 5873.
(43) Horne, R. A. *Water and Aqueous Solutions: Structure, Thermodynamics, and Transport Processes*; John Wiley & Sons: New York, 1972.
(44) Niesar, U.; Corongiu, G.; Huang, M. J.; Dupuis, M.; Clementi, E. *Int. J. Quantum Chem.* **1989**, 421.
(45) Shinoda, W.; Shiga, M. *Phys. Rev. E* **2005**, *71*, 041204.
(46) Che, J.; Cagin, T.; Deng, W.; Goddard, W. A., III. *J. Chem. Phys.* **2000**, *113*, 6888.
(47) Kell, G. S. *J. Chem. Eng. Data* **1967**, *12*, 66.
(48) *Handbook of Chemistry and Physics*, 57th ed.; CRC Press: Cleveland, OH, 1976.
(49) Schenter, G. K. *J. Chem. Phys.* **1998**, *108*, 6222.
(50) Feyereisen, M. W.; Feller, D.; Dixon, D. A. *J. Phys. Chem.* **1996**, *100*, 2993.
(51) Mahoney, M. W.; Jorgensen, W. L. *J. Chem. Phys.* **2001**, *115*, 10758.